

Original Article

# Culex and Aedes Aegypti Detection Model using Convolutional Neural Network and Image Processing Algorithm

Cherry R. Gumiran<sup>1</sup>, Joel M. Gumiran<sup>2</sup>

<sup>1,2</sup>Isabela State University, Philippines.

<sup>1</sup>Corresponding Author : [cherry.r.gumiran@isu.edu.ph](mailto:cherry.r.gumiran@isu.edu.ph)

Received: 27 October 2024

Revised: 08 July 2025

Accepted: 16 July 2025

Published: 30 July 2025

**Abstract** - Dengue fever is an illness spread by mosquitoes. The disease became widespread worldwide as the number of reported cases increased year after year, especially in the Philippines, which had the highest number of infected patients in Asia in 2019. As a consequence, according to the press, many projects have been initiated and adopted. As a result, these were effectively addressed, but they should be followed religiously for long-term effect. As a result, automated technology has been integrated to identify the mosquito carrier's position effectively, referred to as mapping using AI, GIS, Fuzzy Logic, and CNN. However, images used in the previous studies are in static parts with no other species combined in them. Hence, images are practically clean and easy to segment and classify. IN contrast, these insects will mature and propagate. Thus, this paper proposes an automatic classification for living and moving Aedes and Culex, combined with other living organisms like different types of insects, dirt or soil, larvae, and different kinds of mosquitoes. This paper used six various pre-processing methodologies for cleaning the images, combined with the Convolutional Neural Network. There are seven layers used in CNN, which comprise Relu, Inception, max-pooling, and resizing. The generated model, images had reached 92.83 percent of validation accuracy rate, which thus proves the success rate of a CNN and the pre-processing.

**Keywords** - Aedes Aegypti, Culex, CNN, Image detection, Image processing.

## 1. Introduction

Dengue is a mosquito-borne viral infection that has become endemic in more than 100 countries worldwide, according to the World Health Organization (WHO). In 2019, the Philippines alone reported the highest cases across Asia, where 420,000 patients were informed [1, 2]. Like Culex, a mosquito species carrying the parasites, killed thousands of penguins in South Africa [3]. As a result, the WHO mandated prevention and control methods to combat the mosquito vectors. These include, but are not limited to, eliminating the mosquito breeding sites, personal protection against mosquito bites, community engagement, reactive vector control, and active mosquito and virus surveillance. With the surging cases of dengue, the Philippine government initiated and implemented various programs such as the “4 o’clock habit”, the “4 s kontra Dengue”, “Clean up Drive,” “Spraying Operation,” “Mapping of Infected cases” [4], and utilizing the Ovitrap of the Department of Science and Technology (DOST). Hence, breeding sites were successfully eradicated with the active cooperation of community engagement and reactive vector control. Thus, reported cases were effectively mitigated with a decrease of 66% by the end of 2020 [5]. However, these programs should be observed religiously to

achieve a long-term impact on society and prevent dengue outbreak recurrence.

Through DOST, the Philippines’ science and technology arm has developed devices to contain the spread of dengue-carrying mosquitoes via the Ovitrap. Ovitrap or OL trap are black containers filled with water and substrates where mosquitoes can lay their eggs. These Ovitrap were installed in random places, and data are reported weekly or monthly, depending on the weight of the data gathered, to the nearest Research Laboratory for analysis. So, the time spent transporting and analyzing data manually, finding dengue carriers, is inefficient. Also, local government units (LGUs) affect response time when addressing the problem.

Furthermore, various approaches have been adopted to solve the challenge mentioned above, including Artificial Intelligence (AI) [5, 6], Geographic Information Systems (GIS) [7, 8], and Fuzzy Logic [9]. Accordingly, Fuzzy Logic is being used in numerous research studies and has proven to be successful in mapping or categorizing mosquito types [8] or data input dependent [7, 9]. Meanwhile, the Geographical Information System (GIS) is being utilized to locate dengue-infected mosquito breeding sites. Survey questions were used,



and the data gathered were used for mapping [10]. However, due to the procedure's epidemiological component, the indices employed were confined to their area, and the data obtained may not be adequate for prediction. A Convolutional Neural Network has also been introduced, primarily for categorizing mosquito larvae [7]. CNN excels at picture classification in manually recorded photos taken with a microscope.

Therefore, pictures were anticipated to be partly clean, with new backgrounds and no moving insects. So, it is simple to examine and classify [7]. Conversely, actual pictures recorded in the field are difficult to classify, especially when combined with other creatures such as bacteria or soil and different mosquitoes, eggs, and insects. As a result, the images captured may be in different positions due to movement, blurry due to water quality, or a mix of both. Categorization is thus both a task and a problem to overcome. Unfortunately, this approach is carried out inefficiently, resulting in maturation and propagation. So, the purpose of this study is to develop a model that will automatically detect adult mosquitoes, particularly *Culex* and *Aedes aegypti*, through segmentation and classification, integrating the Convolutional Neural Network and Image Processing Algorithm.

## 2. Review of Related Literature

Images are now commonly used for analysis, particularly in diseases affecting humans, plants [11-13], animals [14], and insects [15, 16]. Identifying conditions in humans and animals necessitates specialized and expensive equipment such as CT scans, ultrasound, etc. As a result, generating results will be delayed and costly in this manner. Several approaches and procedures have been published and applied to achieve the same performance as professionals and high-end devices using the image classification technique.

According to the evaluation, these approaches were also expanded to various types, comparable to what was stated, and provided efficient and successful outcomes. [11, 12, 15, 16]. Convolutional Neural Network (CNN), Artificial Neural Network (ANN), Support Vector Machine (SVM), K-nearest Neighbors (KNN), and Naive-Bayes (NB) are widely used for image classification [15].

According to research, machine learning algorithms, specifically convolutional neural network models, have the highest accuracy classification rate of 91.5 percent for 9 and 24 insect groups from the provided dataset for insect classification [15]. Aside from that, CNN demonstrated its efficacy in effectively supplying the presence of cherries for grading [17] and in teaching from controlled training imagery in classifying and quantifying areas within plot-level imagery as symptomatic, asymptomatic, or ground [18]. The pixels, such as edges, textures, colors, and others, are extracted by the layer on the convolutional network, identified as its power in image processing [19]. On the other hand, the convolutional neural

network is prone to overfitting due to its massive number of parameters and feature complexity [19, 20]. However, in this manner, the pre-processing technique is also essential to get an accurate result, which includes masking [21-23] filtering [23, 24], applying thresholding [11, 25, 26], edge detection algorithm [27, 28], and max-pooling [31, 32]. Masking has been shown in studies to increase the classification of celiac versus control images to about 80% accuracy, compared to 70-77 percent without masking.

According to previous research, celiac disease patients had lower mean pixel brightness and higher variability in brightness, and further masking was needed to eliminate extraneous features. As a result, color masking was discovered to help eliminate the dim features from the imaged video capsule. It improves classification by separating celiac disease with villous atrophy from a control video capsule file [23]. On the other hand, thresholding was used in the segmentation technique to separate several objects from the context and detect the point of interest from the original image. According to the findings, the optimum thresholding value was used in the SSD algorithm to partition the image into sub-regions. As a result, the leaf folder and yellow stemborer moths were identified [26].

Pooling is the process of removing unwanted objects from images. Furthermore, the primary goal of spatial pooling is to aggregate neighboring descriptors for a given area. To put it another way, it contains the appropriate pieces while eliminating the irrelevant ones. This technique was used in a study by J.I. Forcen et al., which explains why pooling is vital in image classification. According to their research, the approach enhanced the collection of relevant data without compromising the picture classification's discriminative strength [29].


















## 3. Materials and Methods

### 3.1. Data Sampling

Images were collected from Kaggle.com, which comprises 3,100 images for *Aedes aegypti* and 600 for the *Culex* mosquito. However, 513 were only utilized out of 3,100 for the *Aedes* due to the simulation requirement process, whereas *Culex* remained 600. Also, *Aedes aegypti*, another type of mosquito, has been added, and it was notably used during testing. Furthermore, these images have been captured using this device which is composed of a microcomputer: Raspberry Pi 4 Model B, Quad-core Cortex-A72, and 2GB LPDDR4-3200 SDRAM; A black cylindrical compartment: diameter 12 cm and height 4 cm with a short focal length (2.5 cm; illumination (15 white-colored LEDs – RGB visible light), and background illumination (white color).

In addition, a camera module captured the mosquito pictures. Data were divided into training data, equivalent to 80%, while the test data is 20%. See Table 1 for the sample photos used for the trained and test data.

Table 1. Sample data used for training and testing

Train Data				Test Data	
Aedes aegypti		Culex		Albopictus	
					
					
					
					

### 3.2. Processing Methods

The proposed image processing algorithm for the automatic segmentation and extraction of an adult *Aedes aegypti* and *Culex* consists of 6 pre-processing techniques:

#### 3.2.1. Brightness Adjustment

This procedure was carried out to reveal more details in the mosquito image, leading to improved categorization results. Therefore, in this study, a specific formula was used to adjust the image's brightness and contrast.

$$img2 = img + 90,$$

Where *img* serves as the original picture, while *img2* is the modified version with adjusted brightness. Meanwhile, **90** depicts the amount of pixel intensity is increased, and any values exceeding 255 will saturate at 255, producing a brighter image. In addition, the *im2* has also been adjusted for its contrast using this formula.

$$img2 = imadjust(img, [0 \ 0.5]),$$

Where the *imadjust* is MATLAB, a function used to modify the image contrast. The parameter [0 0.5] defines the input intensity range, where the value 0 corresponds to black and 0.5 represents a mid-gray. These input values are then linearly mapped to cover the full output intensity range from 0 to 1, spanning from black to white. As a result, all pixel

values are normalized between 0 and 0.5 and proportionally stretched across the entire output range between 0 and 1.

#### 3.2.2. Color Conversion: RGB to Grayscale

Converting an RGB image to grayscale significantly impacts the classification process. This conversion is achieved by applying the following pseudo-code, which calculates a weighted sum of the red, green, and blue channels to reflect human brightness perception.

```
imgC = img;
img = rgb2gray(img);
figure;
%img = imread('..\Dataset/Train/Aedes/Aedes (17).jpg');
subplot(2,2,1);
imshow(img);
title('Aedes');
```

Fig. 1 Pseudo code for RGB to gray conversion

Where the original image is stored in the variable *imgC*, it is assigned to *img*. Whereas, the command *img = rgb2gray(img)*; It is specifically used to convert the RGB image to grayscale by eliminating the hue and saturation while preserving the luminance. This function calculates a weighted sum of the red, green, and blue color channels to generate a single intensity value per pixel, effectively transforming the image into shades of gray. Furthermore, the command *subplot(2,2,1)*; arranges the multiple images within a single

figure window by dividing it into 2 rows and 2 columns, and then activates the first subplot position for displaying an image.

### 3.2.3. Histogram Equalizer

This method improves image contrast by expanding the range of intensity values, which enhances the visibility of details in both bright and dark areas. The enhancement is achieved by applying the following formula that redistributes pixel intensities to utilize the full available dynamic range.

$$img2 = histeq(img),$$

Where *img* stores the equalized image, while *histeq(img)* is a MATLAB function that equalizes the picture.

### 3.2.4. Median Filtering

This technique reduces image noise effectively. In this study, it is implemented by integrating it into the pseudo-code, as demonstrated in Figure 2.

```
for(i=1:3)
    img4(:, :, 1) = medfilt2(img2(:, :, 1), [3,3]);
end;
subplot(2,2,3);
imshow(img4);
title('filter');
```

Fig. 2 Pseudo-code applying median filtering

Where the loop iterates three times. During each iteration, *img2(:, :, 1)* extracts the first color channel from the 3D image matrix *img2*. The function *medfilt2(img2(:, :, 1), [3,3])* then applies a 2D median filter with a 3x3 neighborhood to this single channel. This process replaces each pixel with the median value of its 3x3 neighborhood, effectively reducing noise while preserving edges better than averaging filters.

### 3.2.5. Canny Edge Detection

Canny detection delivers more precise and cleaner edge outlines, making it a popular choice in image processing tasks such as object boundary detection and segmentation. This effectiveness is achieved through a multi-stage algorithm that reduces noise, precisely localizes edges, and ensures continuous edge representations, as demonstrated by the formula below.

$$imgfiltercanny = edge(imgtgray, 'canny');$$

Furthermore, this method represents a more advanced edge detection technique that incorporates Gaussian filtering to smooth the image and reduce noise, gradient calculation to identify edge strength and direction, non-maximum suppression to thin edges, and double-thresholding to distinguish strong and weak edges. These steps collectively

produce a cleaner and more accurate edge map. The resulting output, *imgfiltercanny*, is a binary image highlighting the detected edges.

### 3.3. Modeling

A Convolutional Neural Network (CNN) is known for its proficiency in calculating the best-suited value for the image classification process. Hence, this was applied in designing a model for classifying the Aedes and Culex mosquitoes that killed millions of people worldwide and thousands of penguins in South Africa.

This approach includes ten convolutional layers followed by max-pooling layers, Relu, Inception Module, and Global Average Pooling. A max-pooling layer performs down-sampling by dividing the input into rectangular pooling regions and computing the maximum of each part. In this model, the activation function used is the ReLu, whereas the softmax is given as:

$$f(x) = \max(0, x)$$

The softmax function is given as:

$$f(xi) = \sum k \left( \frac{e^{x_i}}{e^{x_k}} \right)$$

Furthermore, the inception module will combine a series of blocks or parameters in a layer to concatenate each block's output, which improves the model's performance. In this manner, this module helps to increase the accuracy of the image classification. At the same time, a global average pooling layer performs down-sampling by computing the mean of the height and width dimensions of the input image. And lastly, a dropout is also added to reduce network overfitting. With the specified pool/kernel size, the same sliding process over the image will be used.

### 3.4. Image Classification and Evaluation

The final process will be where the image has been identified using the created model. Throughout the number of epochs, classification results will be displayed. In this manner, the higher the accuracy rate, the higher the validation of accuracy in the classification process. The classification formula calculates the classification accuracy of the model.

$$Accuracy = \frac{TP+TN}{TP+TN+FN+FP}$$

$$Precision = \frac{TP}{TP+FP}$$

$$Recall = \frac{TN}{TN+FP}$$

$$F1 - Score = \frac{2TP+TN}{2TP+FN+FP}$$



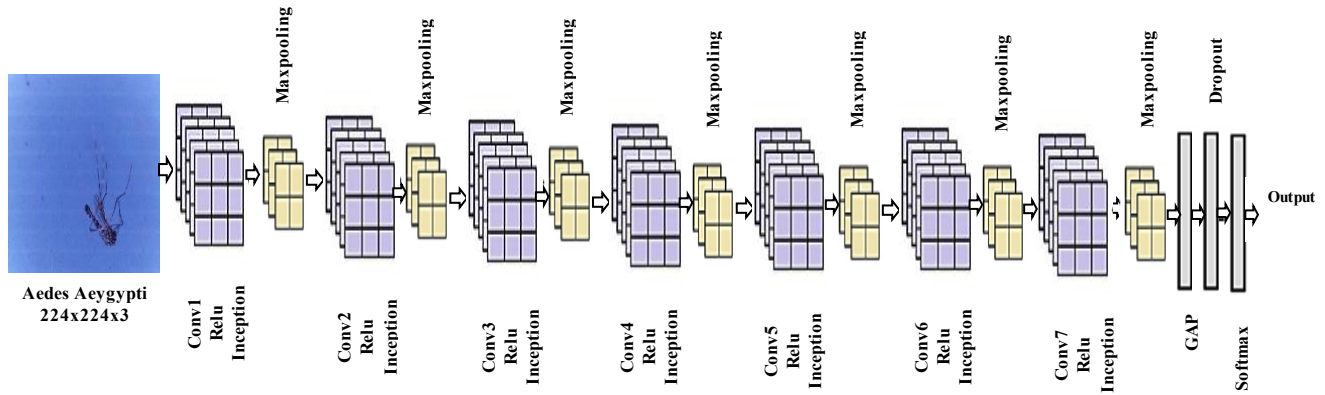


Fig. 3 Aedes and Culex detection model using CNN approach

Where TP represents True Positive, TN, True Negative, FN, False Negative, and FP, False Positive, the result appears in the number of insects based on their category name, Aedes Positive and Aedes Negative. Aedes is positive if the image was detected as Aedes positive; otherwise, it is negative.

In this regard, the accuracy refers to the overall correctness of the classification. At the same time, precision depicts the accuracy of positive predictions. In addition, recall measures the ability to find all positive cases, and the F1-score represents the harmonic mean of precision and recall, balancing both.

## 4. Results and Discussion

### 4.1. Training and Development

Several researchers used high-quality cameras to capture the item and used various approaches for categorizing pictures. The techniques and instruments utilized were deemed to be compelling. However, because the images were taken in a static position with no other species present during the experiment, they are partially clean and easier to separate and categorize.

This approach was thus confined to non-moving objects and used in a pristine setting where positioning and cleaning were not a concern. Therefore, this research proposed demonstrating how to organize moving and living entities, particularly Aedes and Culex, in a crowded habitat that includes other moving and living organisms such as insects, dirt or soil, a different type of mosquito, and larval insects in general.

Images for this experiment were acquired from the Kaggle website, which has items placed in a busy environment and photographed in various positions. The example dataset may be found in Table 1. The MATLAB platform was then used to develop six further pre-processing methods. The transformation of the Aedes aegypti using the stated pre-processing technique is shown in Figure 4.

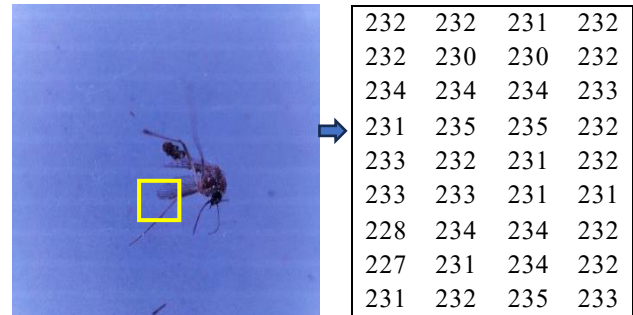


Fig. 4 Raw image with pixel values

### 4.2. Pre-Processing

The initial pre-processing step involved adjusting the brightness. In this approach, 90 units were added to the pixel intensity of the original image, leading to more saturated pixel values, as illustrated in Figure 5(b).

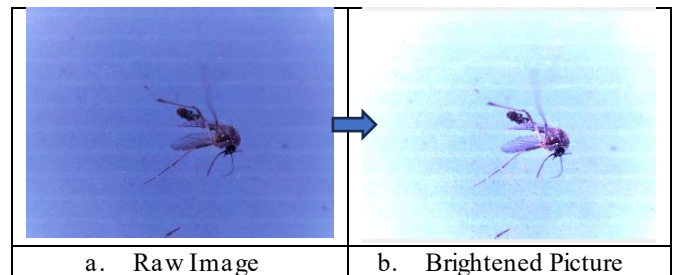
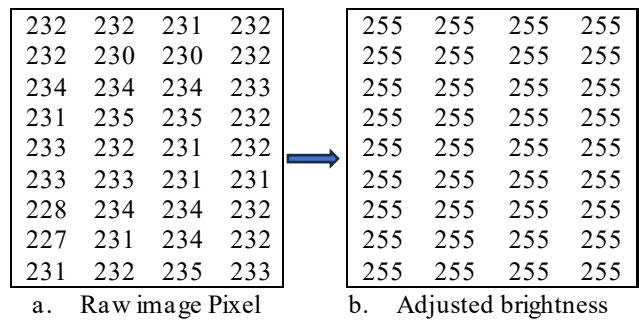
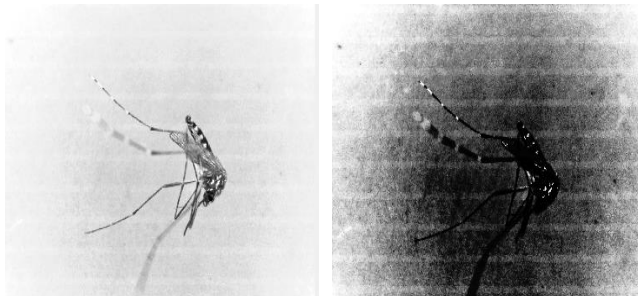


Fig. 5 Pixel transformation applying the brightness adjustment formula

Conversely, some noise became more pronounced; hence, contrast adjustment was applied using the formula  $img2 = imadjust(img, [0 \ 0.5])$ . This process normalizes pixel intensities by linearly mapping values within the input range  $[0, 0.5]$  to the full output range, effectively enhancing contrast while scaling the pixel values proportionally. Despite the proportionate adjustment, segmenting the object from the background remains a challenge, which negatively affects the classification accuracy. Consequently, the brightened picture has been converted to grayscale, transforming the RGB image into two colors: black and white. These two colors effectively represent the background and the mosquito, as illustrated in Figure 6(a).



a. RGB to gray conversion      b. Equalized picture  
Fig. 6 Grayscale transformation

On the contrary, to capture the feature of the mosquito, regions have to be more visible by darkening; thus, an equalization procedure is applied as another pre-processing technique. This equalization enhances contrast by spreading out the intensity values, making the mosquito's edges more distinct, as shown in Figure 6(b). However, this also darkens the background, complicating the segmentation of the mosquito from its surroundings. To address this, another pre-processing technique was implemented: Median filtering.

Median filtering is employed to reduce noise in images. In this study, the filtering technique is applied through pseudo-code that uses a 3x3 neighborhood on a single color channel. This method replaces each pixel's value with the median of the surrounding 3x3 pixel values, effectively suppressing noise while preserving important edges and details better than averaging filters.

247	247	243	247
247	247	247	247
243	243	239	247
239	235	239	247
239	239	243	243
247	239	235	247
223	239	243	239
231	231	235	235

a. Pixel value of the equalized image

247	247	247	243	247	247
247	247	247	243	247	247
247	247	247	247	247	247
243	243	243	239	247	247
239	239	235	239	247	247
239	239	239	243	243	243
247	247	239	235	247	247
223	223	239	243	239	239
231	231	231	235	235	235
231	231	231	235	235	235

b. Applying pixel explorations

247	247	247	243	247	247
247	247	247	243	247	247
247	247	247	247	247	247
243	243	243	239	247	247
239	239	235	239	247	247
239	239	239	243	243	243
247	247	239	235	247	247
223	223	239	243	239	239
231	231	231	235	235	235
231	231	231	235	235	235

c. 3 x 3 masking

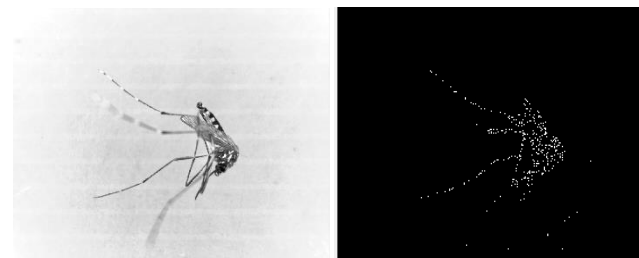
247	247	247	243	247	247
247	247	247	243	247	247
247	247	247	247	247	247
243	243	243	247	247	247
239	239	235	239	247	247
239	239	239	243	243	243
247	247	239	235	247	247
223	223	239	243	239	239
231	231	231	235	235	235
231	231	231	235	235	235

d. Applying pixel exploration

e. Median filtering

Fig. 7 Pixel transformation using median filtering

As shown in Figure 7(e), some pixels remained unchanged, while others were altered. This process cleared the noise from the background, making the mosquito more prominent. In the figure, the highlighted red indicates those that stayed the same, whereas the highlighted green represents those that changed after applying the median filtering. Following this, Canny edge detection was employed to highlight the mosquito's edge and regions, as illustrated in Figure 8(b).



a. Applying median filtering

b. Applying canny edge detection

Fig. 8 Image transformation

It was discovered that pictures were free of extraneous sounds that interfered with classification by employing the approach mentioned above. Furthermore, parameters were modified during the testing, notably on the brightness and brightening of the gray. In this way, the luminance was determined to be 0.5 weight, while the gray image's brightness was also increased to 2. Additionally, due to the image's noise, median filtering has been performed. Similarly, canny edge detection eliminates the background by darkening it and leaving only the insect.



**Table 2. Testing the classification model**

Test	Classifying Aedes Aegypti			
	Accuracy	Precision	Recall	F1-Score
1	95.41	60.91	8.34	14.68
2	94.72	10.90	1.62	2.83
3	94.84	21.31	3.33	5.76
Classifying Culex				
1	93.32	12.44	6.82	8.81
2	92.41	11.05	8.56	9.64

Moreover, the model's performance in classifying the mosquito using the individual image is illustrated. Three (3) tests were conducted to compare the application of the pre-processing technique and exclude it from the process.

As shown in the table, the model demonstrates significant effectiveness in the classification process, particularly in

identifying individual objects. It achieved a maximum accuracy of 95.41% when classifying Aedes mosquitoes, with a precision of 60.91 percent, a recall of 8.34 percent, and an F1-score of 14.68 percent. In contrast, the classification of Culex mosquitoes reached a maximum accuracy of 93.32 percent, with a precision of 12.44 percent, a recall of 6.82 percent, and an F1-score of 8.81 percent.

## 5. Conclusion

The prediction rate of classifying the adult Aedes aegypti mosquito achieved its highest accuracy rate of 92 percent during the experiment using the collected images from Kaggle and the produced model, which is lower than the insect's classification rate [14], which is equal to 83 percent. As a result, the photographs were used to execute the model effectively. On the other hand, to determine its precision, this model would use actual data from the field.

## References

- [1] Philippines: Dengue Cases Down 36 Percent so Far in 2020 - Outbreak News Today. [Online]. Available: <http://outbreaknewstoday.com/philippines-dengue-cases-down-36-percent-so-far-in-2020/>
- [2] Frances Mangosing, and Katrina Hallare, BREAKING: DOH Declares National Dengue Epidemic, INQUIRER.net, 2019. [Online]. Available: <https://newsinfo.inquirer.net/1150828/breaking-doh-declares-national-dengue-epidemic>
- [3] Philippines Dengue Cases Down 66% in 2020 - Outbreak News Today. [Online]. Available: <http://outbreaknewstoday.com/philippines-dengue-cases-down-66-in-2020/>
- [4] Antonio Arista-Jalife et al., "Aedes Mosquito Detection in its Larval Stage Using Deep Neural Networks," *Knowledge-Based Systems*, vol. 189, 2020. [CrossRef] [Google Scholar] [Publisher Link]
- [5] Faiz Madzlan et al., "Breeding Characteristics of Aedes Mosquitoes in Dengue Risk Area," *Procedia-Social and Behavioral Sciences*, vol. 234, pp. 164-172, 2016. [CrossRef] [Google Scholar] [Publisher Link]
- [6] Shuchi Mala, and Mahesh Kumar Jat, "Geographic Information System Based Spatio-Temporal Dengue Fever Cluster Analysis and Mapping," *The Egyptian Journal of Remote Sensing and Space Science*, vol. 22, no. 3, pp. 297-304, 2019. [CrossRef] [Google Scholar] [Publisher Link]
- [7] Yane Duan et al., "Automatic Segmentation Method for Live Fish Eggs Microscopic Image Analysis," *Aquacultural Engineering*, vol. 85, pp. 49-55, 2019. [CrossRef] [Google Scholar] [Publisher Link]
- [8] A.N. Babu et al., "Smartphone Geospatial Apps for Dengue Control, Prevention, Prediction, and Education: MOSapp, DISapp, and the Mosquito Perception Index (MPI)," *Environmental Monitoring and Assessment*, vol. 191, no. S1, pp. 1-17, 2019. [CrossRef] [Google Scholar] [Publisher Link]
- [9] Zoe Meleo-Erwin et al., "Readability of Online Dengue Materials: The Need for Accessible Information as Part of Infectious Disease Prevention and Control Efforts," *Infection, Disease & Health*, vol. 25, no. 4, pp. 277-282, 2020. [CrossRef] [Google Scholar] [Publisher Link]
- [10] Alexandre A. Bernardes et al., *Identification of Foliar Diseases in Cotton Crop*, Topics in Medical Image Processing and Computational Vision, Springer, Dordrecht, pp. 67-85, 2013. [CrossRef] [Google Scholar] [Publisher Link]
- [11] Chiranjeevi Muppala, and Velmathi Guruviah, "Detection of Leaf Folder and Yellow Stemborer Moths in the Paddy Field Using Deep Neural Network with Search and Rescue Optimization," *Information Processing in Agriculture*, vol. 8, no. 2, pp. 350-358, 2021. [CrossRef] [Google Scholar] [Publisher Link]
- [12] Vaibhav Tiwari, Rakesh Chandra Joshi, and Malay Kishore Dutta, "Dense Convolutional Neural Networks Based Multiclass Plant Disease Detection and Classification Using Leaf Images," *Ecological Informatics*, vol. 63, 2021. [CrossRef] [Google Scholar] [Publisher Link]
- [13] Likhith Prudhivi et al., "WITHDRAWN: Animal Species Image Classification," *Materials Today: Proceedings*, 2021. [CrossRef] [Google Scholar] [Publisher Link]
- [14] Thenmozhi Kasinathan, Dakshayani Singaraju, and Srinivasulu Reddy Uyyala, "Insect Classification and Detection in Field Crops Using Modern Machine Learning Techniques," *Information Processing in Agriculture*, vol. 8, no. 3, pp. 446-457, 2021. [CrossRef] [Google Scholar] [Publisher Link]
- [15] Midori Tuda, and Alejandro Isabel Luna-Maldonado, "Image-Based Insect Species and Gender Classification by Trained Supervised Machine Learning Algorithms," *Ecological Informatics*, vol. 60, 2020. [CrossRef] [Google Scholar] [Publisher Link]



- [16] Mohammad Momeny et al., "Accurate Classification of Cherry Fruit Using Deep CNN Based on Hybrid Pooling Approach," *Postharvest Biology and Technology*, vol. 166, 2020. [[CrossRef](#)] [[Google Scholar](#)] [[Publisher Link](#)]
- [17] James W. Clohessy et al., "Development of A High-Throughput Plant Disease Symptom Severity Assessment Tool Using Machine Learning Image Analysis and Integrated Geolocation," *Computers and Electronics in Agriculture*, vol. 184, 2021. [[CrossRef](#)] [[Google Scholar](#)] [[Publisher Link](#)]
- [18] Yang Li, Jing Nie, and Xuewei Chao, "Do We Really Need Deep CNN for Plant Diseases Identification?," *Computers and Electronics in Agriculture*, vol. 178, 2020. [[CrossRef](#)] [[Google Scholar](#)] [[Publisher Link](#)]
- [19] Qi Xu et al., "Overfitting Remedy by Sparsifying Regularization on Fully-Connected Layers of CNNs," *Neurocomputing*, vol. 328, pp. 69-74, 2019. [[CrossRef](#)] [[Google Scholar](#)] [[Publisher Link](#)]
- [20] Yexin Duan et al., "Mask-Guided Noise Restriction Adversarial Attacks for Image Classification," *Computers & Security*, vol. 100, 2021. [[CrossRef](#)] [[Google Scholar](#)] [[Publisher Link](#)]
- [21] Edward J. Ciaccio et al., "Color Masking Improves Classification of Celiac Disease in Videocapsule Endoscopy Images," *Computers in Biology and Medicine*, vol. 106, pp. 150-156, 2019. [[CrossRef](#)] [[Google Scholar](#)] [[Publisher Link](#)]
- [22] Kriti, Jitendra Virmani, and Ravinder Agarwal, "Effect of Despeckle Filtering on Classification of Breast Tumors Using Ultrasound Images," *Biocybernetics and Biomedical Engineering*, vol. 39, no. 2, pp. 536-560, 2019. [[CrossRef](#)] [[Google Scholar](#)] [[Publisher Link](#)]
- [23] Katia M. Poloni et al., "Brain MR Image Classification for Alzheimer's Disease Diagnosis Using Structural Hippocampal Asymmetrical Attributes from Directional 3-D Log-Gabor Filter Responses," *Neurocomputing*, vol. 419, pp. 126-135, 2021. [[CrossRef](#)] [[Google Scholar](#)] [[Publisher Link](#)]
- [24] Ashish Issac, M. Partha Sarathi, and Malay Kishore Dutta, "An Adaptive Threshold-Based Image Processing Technique for Improved Glaucoma Detection and Classification," *Computer Methods and Programs in Biomedicine*, vol. 122, no. 2, pp. 229-244, 2015. [[CrossRef](#)] [[Google Scholar](#)] [[Publisher Link](#)]
- [25] Jose Luis Garcia-Arroyo, and Begonya Garcia-Zapirain, "Segmentation of Skin Lesions in Dermoscopy Images Using Fuzzy Classification of Pixels and Histogram Thresholding," *Computer Methods and Programs in Biomedicine*, vol. 168, pp. 11-19, 2019. [[CrossRef](#)] [[Google Scholar](#)] [[Publisher Link](#)]
- [26] D. Marmanis et al., "Classification with an Edge: Improving Semantic Image Segmentation with Boundary Detection," *ISPRS Journal of Photogrammetry and Remote Sensing*, vol. 135, pp. 158-172, 2018. [[CrossRef](#)] [[Google Scholar](#)] [[Publisher Link](#)]
- [27] Mehdi Fatan, Mohammad Reza Daliri, and Alireza Mohammad Shahri, "Underwater Cable Detection in the Images Using Edge Classification Based on Texture Information," *Measurement*, vol. 91, pp. 309-317, 2016. [[CrossRef](#)] [[Google Scholar](#)] [[Publisher Link](#)]
- [28] J.I. Forcén et al., "Learning Ordered Pooling Weights in Image Classification," *Neurocomputing*, vol. 411, pp. 45-53, 2020. [[CrossRef](#)] [[Google Scholar](#)] [[Publisher Link](#)]
- [29] Huseyin Uzen, Muammer Turkoglu, and Davut Hanbay, "Texture Defect Classification with Multiple Pooling and Filter Ensemble Based on Deep Neural Network," *Expert Systems with Applications*, vol. 175, 2021. [[CrossRef](#)] [[Google Scholar](#)] [[Publisher Link](#)]